

Similarities between optimal precursors for ENSO events and optimally growing initial errors in El Niño predictions

Mu Mu · Yanshan Yu · Hui Xu · Tingting Gong

Received: 13 September 2012 / Accepted: 16 April 2013 / Published online: 1 May 2013
© Springer-Verlag Wien 2013

Abstract With the Zebiak–Cane model, the relationship between the optimal precursors (OPR) for triggering the El Niño/Southern Oscillation (ENSO) events and the optimally growing initial errors (OGE) to the uncertainty in El Niño predictions is investigated using an approach based on the conditional nonlinear optimal perturbation. The computed OPR for El Niño events possesses sea surface temperature anomalies (SSTA) dipole over the equatorial central and eastern Pacific, plus positive thermocline depth anomalies in the entire equatorial Pacific. Based on the El Niño events triggered by the obtained OPRs, the OGE which cause the largest prediction errors are computed. It is found that the OPR and OGE share great similarities in terms of localization and spatial structure of the SSTA dipole pattern over the central and eastern Pacific and the relatively uniform thermocline depth anomalies in the equatorial Pacific. The resemblances are possibly caused by the same mechanism of the Bjerknes positive feedback. It implies that if additional observation instruments are deployed to the targeted observations with limited coverage, they should preferentially be deployed in the equatorial central and eastern Pacific, which has been determined as the sensitive area for ENSO prediction, to better detect the early signals for ENSO events and reduce the initial errors so as to improve the forecast skill.

1 Introduction

The El Niño/Southern Oscillation phenomenon (ENSO) is one of the strongest modes of the climate variability on interannual time scales. Although ENSO occurs in the tropical Pacific Ocean, where strong sea surface temperature anomalies (SSTA) are observed, it affects climate, societies in many regions of the world (Philander 1990). Hence, an accurate prediction of ENSO onset is of vital importance for short-term climate prediction in terms of precipitation and temperature. One focus of dynamic meteorology research is to address the nature of the initial perturbations that is most likely to develop into weather or climate events we are interested in. This initial perturbation, under some conditions, is called as the optimal precursor (OPR) to the weather or climate event. Finding the OPR that evolves into an ENSO event will help us understand the process of ENSO onset and improve the prediction skills (Blumenthal 1991; Xue et al. 1994, 1997a, b; Moore and Kleeman 1996, 1997a, b; Chen et al. 1997; Thompson 1998). Moore et al. (2003) reviewed some important mathematical methods pertaining to the optimal perturbations, such as the most unstable eigenmode, adjoint eigenmode, and the fastest growing singular vector. However, these methods are based on the linear assumption and become limited when the nonlinear effects are taken into account. Xue et al. (1997a, b) also pointed out that the nonlinear advection processes contribute significantly to the asymmetry of ENSO behavior. Mu et al. (2003) developed a nonlinear method to study the predictability of ENSO, which is an extension of a singular vector in the nonlinear regime, called conditional nonlinear optimal perturbation (CNOP). Duan et al. (2004) used this method and a simple theoretical model to identify the optimal perturbations (i.e., CNOPs) corresponding to El Niño and La Niña events, respectively. They investigated the effects of nonlinearity on the asymmetry evolutions of CNOPs related to El Niño and La Niña events through a comparison between CNOP and the fastest growing singular vector. Xu (2006) also applied this

M. Mu · Y. Yu · T. Gong (✉)
Key Laboratory of Ocean Circulation and Wave,
Institute of Oceanology, Chinese Academy of Sciences,
Qingdao 266071, China
e-mail: ttg@qdio.ac.cn

H. Xu
LASG, Institute of Atmospheric Physics, Chinese Academy
of Sciences, Beijing 100029, China

method to find the optimal perturbations that evolve into El Niño and La Niña events in the context of the intermediate complexity Zebiak–Cane model (1987).

Although significant progresses on searching the OPR for ENSO events have been achieved, it is not always capable to capture the OPR in the analysis field in advance to forecast whether an ENSO event will take place. Not only because the magnitude of the OPR is very small to identify, but also the lack of full coverage of SST measurement would cause significant initial errors existing along with the OPR and might destroy the forecast results. Therefore, the determination of initial error that leads to the greatest loss of forecast skill will help us find out the sources of prediction errors, which is also a main aspect of ENSO predictability study. This initial error, which causes the largest prediction error under a given constraint, is denoted as the optimally growing initial error (OGE) in this study. Xue et al. (1997a, b) considered the fastest growing singular vector around ENSO cycle as OGE and found its dominant growing structure, characterized by north–south and east–west SST dipoles, convergent winds on the equator in the eastern Pacific, and a deepened thermocline in the whole equatorial belt. This structure is insensitive to the start month or the optimization time. Note that the singular vector method has also been widely used in other predictability studies besides ENSO predictability (Lorenz 1965; Buizza and Palmer 1995). For synoptic scale circulations, the largest singular value can be used as an appropriate warning of uncertainties in numerical weather prediction. More realistic ensemble forecasts are now being constructed using the fastest growing singular vectors as initial perturbations in numerical weather forecasts at the European Centre for Medium-Range Weather Forecasts (Mureau et al. 1993; Molteni et al. 1996). To consider the nonlinear effects, Mu et al. (2007) used the CNOP method to find OGE in ENSO predictions, and investigate their effects on a phenomenon called as “spring predictability barrier.” Furthermore, Yu et al. (2009) pointed out that these OGEs computed with the CNOP method can be classified into two types: one possessing an SSTA pattern with negative anomalies over the equatorial central–western Pacific and positive anomalies over the equatorial eastern Pacific, and a positive thermocline depth anomaly pattern along the equator, and the other possessing almost the same pattern but with opposite signs to the former. The former type of OGE tends to overpredict the strength of an El Niño event, while the latter tends to underestimate it. Duan and Wei (2012) further demonstrated that the initial SST errors similar to the structure of the two types of OGEs occur in the ENSO predictions generated by a Flexible Global Ocean–Atmosphere–Land System model (FGOALS-g); furthermore, the errors are also related to a significant SPB for El Niño events. It is inferred that if data assimilation or targeted observation

approaches are used to filter the CNOP-like errors in the predictions generated by the FGOALS-g, the ENSO forecast skill might be greatly improved. It is therefore very useful to investigate the OGE of El Niño prediction.

As it has been stated above, the CNOP is an initial perturbation whose nonlinear evolution attains the maximal value of the cost function (Mu et al. 2003; Mu and Duan 2003; Mu and Zhang 2006). It is a natural generalization of the LSV approach to a nonlinear regime. For short-term climate prediction, CNOP is the initial perturbations that is most likely to develop into weather or climate events we are interested in. In predictability studies, CNOP represents the optimally growing initial error that has the worst effect on the prediction result at the optimization time (Mu et al. 2003). CNOP has therefore been used to identify the optimal initial error that causes the largest prediction error for ENSO events (Xu and Duan 2008), as an attempt to explore the effect of nonlinearity on error growth for ENSO. It is evident that the OPR exists in ENSO onset and the OGE affects the prediction of ENSO onset. However, whether the OPR to ENSO onset and the OGE in onset predictions are related with each other are still undiscovered. Accordingly, we propose the following questions: What are the relationships between the OPR and OGE in ENSO onset predictions? Do the OPR and OGE have similar spatial structures? If these similarities exist, could these relationships provide guidelines for targeted observation and improvement for ENSO event forecasting? To answer these questions in this paper, the OPR and OGE will be calculated with the CNOP method.

The outline of this paper is as follows. In Section 2, we present the nonlinear optimization problem related to the exploration of the OPR and the OGE, the numerical results of the OPR and OGE, and the similarity characteristics between them. Implications of similarities between the OPR and OGE in targeted observation are presented in Section 3. Finally, the main results are summarized and discussed in Section 4.

2 Optimal precursors that trigger ENSO onset and optimally growing initial errors in ENSO prediction

The present numerical experiments employ the ZC model, which is a nonlinear anomaly model of intermediate complexity that describes anomalies about a specified seasonally varying background, avoiding the “climate drift” problem (Zebiak and Cane 1987). The atmosphere model and the prognostic equation of SSTA are run at a horizontal resolution of $5.625^\circ \times 2.0^\circ$. The ocean model is a grid point model with a horizontal resolution of $2.0^\circ \times 0.5^\circ$. The tangent linear and adjoint models of ZC model were developed with code-by-code method by Xu (2006). To solve the nonlinear

optimization problems, these models will be used to provide information to solvers. Specific procedures will be described in detail as follows.

2.1 Optimal precursors that trigger ENSO events

The OPR is the initial perturbation that is most likely to develop into an ENSO event under a given constraint. In order to obtain the OPR from the ZC model, the ZC-specified climatology with the seasonal cycle is used as the basic state. Therefore, the measurement of the likelihood of developing into an ENSO event is determined by the departure of the initial perturbation evolution from the seasonal cycle at the end of optimization time interval. Because onset times of ENSO events do not always lie in a particular month, we seek the OPRs corresponding to 4 months, January, April, July, and October. Assuming that the initial perturbations exist in SST and thermocline depth, the OPR computed by CNOP method consists of two components: the SSTA and the thermocline depth anomaly. To obtain the OPR, a cost function is constructed to measure the evolution of the initial perturbation of SST at the end of optimization time interval. The CNOP, denoted by $u_{0\delta}$, is obtained by solving the following nonlinear optimization:

$$J(\bar{u}_{0\delta}) = \max_{\|\bar{u}_0\|_1 \leq \delta} \|\bar{T}'(\tau)\|_2, \tag{1}$$

where $\bar{u}_0 = (w_1^{-1}\bar{T}'_0, w_2^{-1}\bar{h}'_0)$ is a non-dimensional initial SSTA and thermocline depth anomaly perturbation superimposed on the initial state of seasonal cycle. $w_1 = 2^\circ\text{C}$ and $w_2 = 50\text{ m}$ are the characteristic scales of the SST and the thermocline depth. The constraint condition, $\|\bar{u}_0\|_1 \leq \delta$, is defined by a prescribed positive real number δ and the norm

$$\|\bar{u}_0\|_1 = \sqrt{\sum_{i,j} \left[(w_1^{-1}T'_{0i,j})^2 + (w_2^{-1}h'_{0i,j})^2 \right]}, \text{ where } T'_{0i,j}$$

and $h'_{0i,j}$ represent the dimensional initial SSTA and thermocline depth anomaly at different grid points and (i, j) is the interior grid point in the domain of the tropical Pacific ($135^\circ\text{ E} - 90^\circ\text{ W}$ by 5.625° ; $17^\circ\text{ S} - 17^\circ\text{ N}$ by 2°). The cost function is the evolution of the initial SSTA at time τ , measured by $\|\bar{T}'(\tau)\|_2 = \sqrt{\sum_{i,j} T'_{ij}(\tau)^2}$. $\bar{T}'(\tau)$ represents the SSTA at time τ , obtained directly by integrating the ZC model through time τ .

The CNOP can be computed by using the Spectral Projected Gradient 2 algorithm, which is used to solve the nonlinear minimization problems with equality and/or inequality constraint condition. A detailed description is given by Birgin et al. (2000).

The initial times are January, April, July, and October and the time interval is one year. The constraint bound δ related to the CNOP perturbations was predetermined experimentally to be 1.0, indicating that the perturbations of SSTA and

thermocline depth anomaly measured by the chosen norm do not exceed 1.0 (dimensional SSTA 2°C and thermocline depth anomaly 50 m, respectively). Mathematically, CNOP makes the objective function attain the global maximum in the phase space. In some cases, there exists local maximum of the objective function, and the corresponding initial perturbations are referred to local CNOP. The local CNOP perturbations for a given optimization experiment, which causes the second largest departure from the basic state (i.e., La Niña onset), has a spatial pattern similar to that of the CNOP perturbations, but with an opposite sign. In our experiments, for each initial time, i.e., January, April, July, and October, there exists CNOP and local CNOP perturbations which correspond to the precursors for El Niño and La Niña onset, respectively. As a result, the obtained OPRs for different initial times all have shown very similar spatial structures. Therefore we simply take the ensemble mean of these obtained OPRs and present the composite OPRs for El Niño and La Niña, respectively (Fig. 1). It can be seen that the composite SSTA components always have a localized structure over the tropical Pacific, whereas the thermocline depth anomalies tend to be more zonally spread and uniform in the equatorial Pacific. Specifically, the composite OPRs for El Niño events comprise negative SSTA perturbations over the equatorial central Pacific and positive SSTA over the equatorial eastern Pacific, plus positive thermocline depth perturbations in the entire equatorial Pacific (Fig. 1a). The composite OPRs for La Niña events have very similar spatial structures to the former, but with opposite sign (Fig. 1b), causing the decrease of the Niño-3 index and La Niña development.

The physics of the OPRs can be explained by the Bjerknes positive feedback (Duan et al. 2004). Due to the contribution of the annual mean states, e.g., the shallow annual mean thermocline in the eastern Pacific, it favors the feedback between the thermocline and the sea surface temperature by means of upwelling or downwelling. Meanwhile, the specific dipole structure of the OPR induces the zonal wind anomalies over the equatorial Pacific, acting as a trigger of the Bjerknes positive feedback. Weaker (stronger) easterly trade winds over the dipole induce downwelling (upwelling) Kelvin waves that act to weaken (intensify) the upwelling in the equatorial eastern Pacific, where the deepening (shoaling) of the thermocline depth anomalies in the eastern Pacific is favorable for the entrainment of warm surface water (cold subsurface water), leading to an enhanced warm (cold) SSTA in this area. Consequently, the positive (negative) SSTA signal in the Niño-3 region is amplified, causing a significant increase (decrease) of the Niño-3 indices and resulting in the development of El Niño (La Niña) events.

Figure 2 shows the time evolutions of the SSTA component with lead times of 3, 6, 9, and 12 months for the OPR-triggered El Niño and La Niña events with the starting

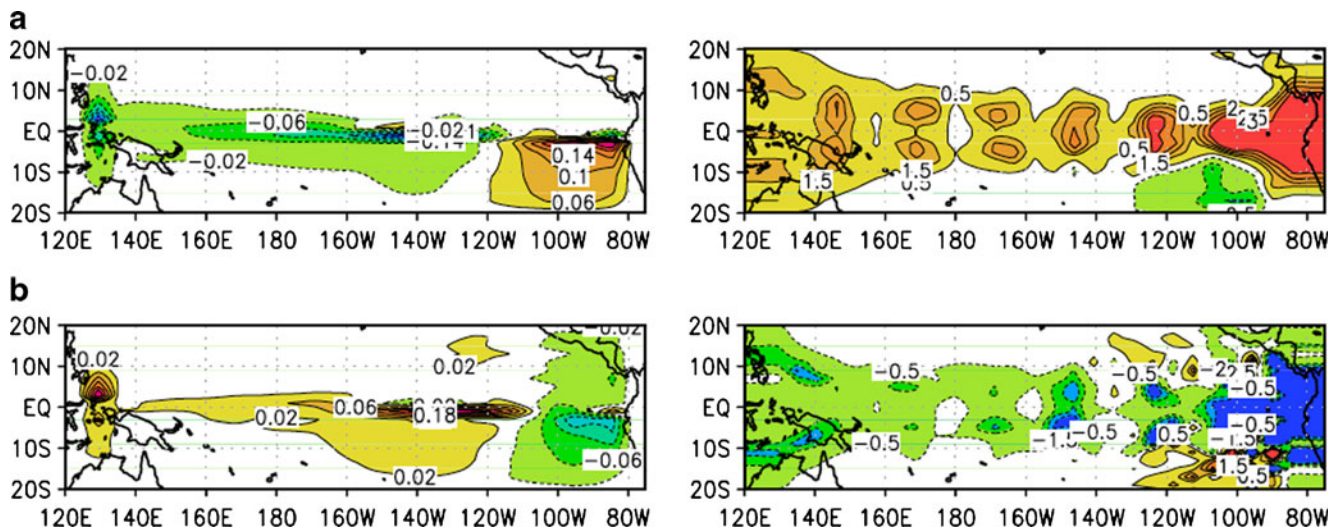


Fig. 1 The composite CNOP (a) and local CNOP (b) precursors with SSTA (left) and thermocline depth anomalies (right)

month being January. The evolution of SSTA in Fig. 2a (b) shows that the positive (negative) SSTA over the equatorial eastern Pacific develop strongly with time, while the negative (positive) SSTA over the central and western Pacific decay gradually and disappear after 3 months, replaced by the intensified positive (negative) SSTA. The dramatic increase in the magnitude of the SSTA suggests that initial anomaly modes with OPR-like spatial structures are most likely to evolve into an El Niño/La Niña event.

2.2 Optimally growing initial errors in El Niño predictions

Upon the above OPRs there remains a special kind of initial error, which causes the largest prediction errors under a given constraint. Finding such optimally growing initial errors (i.e., OGEs) is likely to help us capture the sensitive area of ENSO predictions and improve the accuracy of ENSO predictions by decreasing the initial analysis error in sensitive areas. In this subsection, the El Niño events triggered by the above OPRs are chosen as the basic state to seek the OGEs. Since the ZC model have phase-locking problem in La Niña simulation, we do not focus on the OGEs related to the OPRs for La Niña events. For the above OPRs identified for 4 months (i.e., January, April, July, and October), it is found that the El Niño onsets take place approximately 6 months after the OPRs (not shown). Therefore, we make the predictions for 12 months (i.e., a lead time of 12 months) from 6 consecutive start months after the OPR by superimposing initial errors on the basic state. For instance, for an El Niño event with obtained OPR on January, six predictions are made on February, March, April, May, June and July, for which the start months are chosen to be as long as 5 months before the El Niño onset time. Note that the selected El Niño events are considered as

“true” states and that our research is based on the assumption of a perfect model.

For each prediction experiment, we seek the optimally growing error (i.e., CNOP error) that causes the largest departure from the basic state at the prediction time. To obtain the CNOP error, a cost function is constructed to measure the evolution of the initial error of SSTA. The CNOP error can be obtained by solving the same nonlinear optimization as Eq. (1), where this $\bar{u}_0 = (w_1^{-1}\bar{T}'_0, w_2^{-1}\bar{h}'_0)$ is the initial error superimposed on the initial state of a predetermined reference state El Niño event. The constraint condition, $\|\bar{u}_0\|_1 \leq \delta$, is defined by a prescribed positive real number δ and the norm

$$\|\bar{u}_0\|_1 = \sqrt{\sum_{i,j} \left[\left(w_1^{-1}T'_{0ij} \right)^2 + \left(w_2^{-1}h'_{0ij} \right)^2 \right]}$$

and h'_{0ij} represents the initial error of the SSTA and thermocline depth anomaly at different grid points and (i, j) is the interior grid point in the domain of the tropical Pacific (135° E–90° W by 5.625°; 17° S–17° N by 2°). The cost function is the prediction error of SSTA at time τ , measured by $\|\bar{T}(\tau)\|_2 = \sqrt{\sum_{i,j} T'_{ij}(\tau)^2}$. $\bar{T}'(\tau)$ represents the prediction error of SSTA at time τ obtained by subtracting the SSTA of the reference state from the predicted SSTA at prediction time τ .

For a given optimization experiment, there exists both global CNOP and local CNOP errors which cause the global maximum of objective function and the local maximum in the phase space, respectively. As a result, a total of 24 global CNOP errors and 24 local CNOP errors are obtained from six start months for four OPRs of El Niño events. The constraint bound δ related to the CNOP error was predetermined experimentally to be 1.0, indicating that the initial errors of SSTA and thermocline depth anomaly measured by the

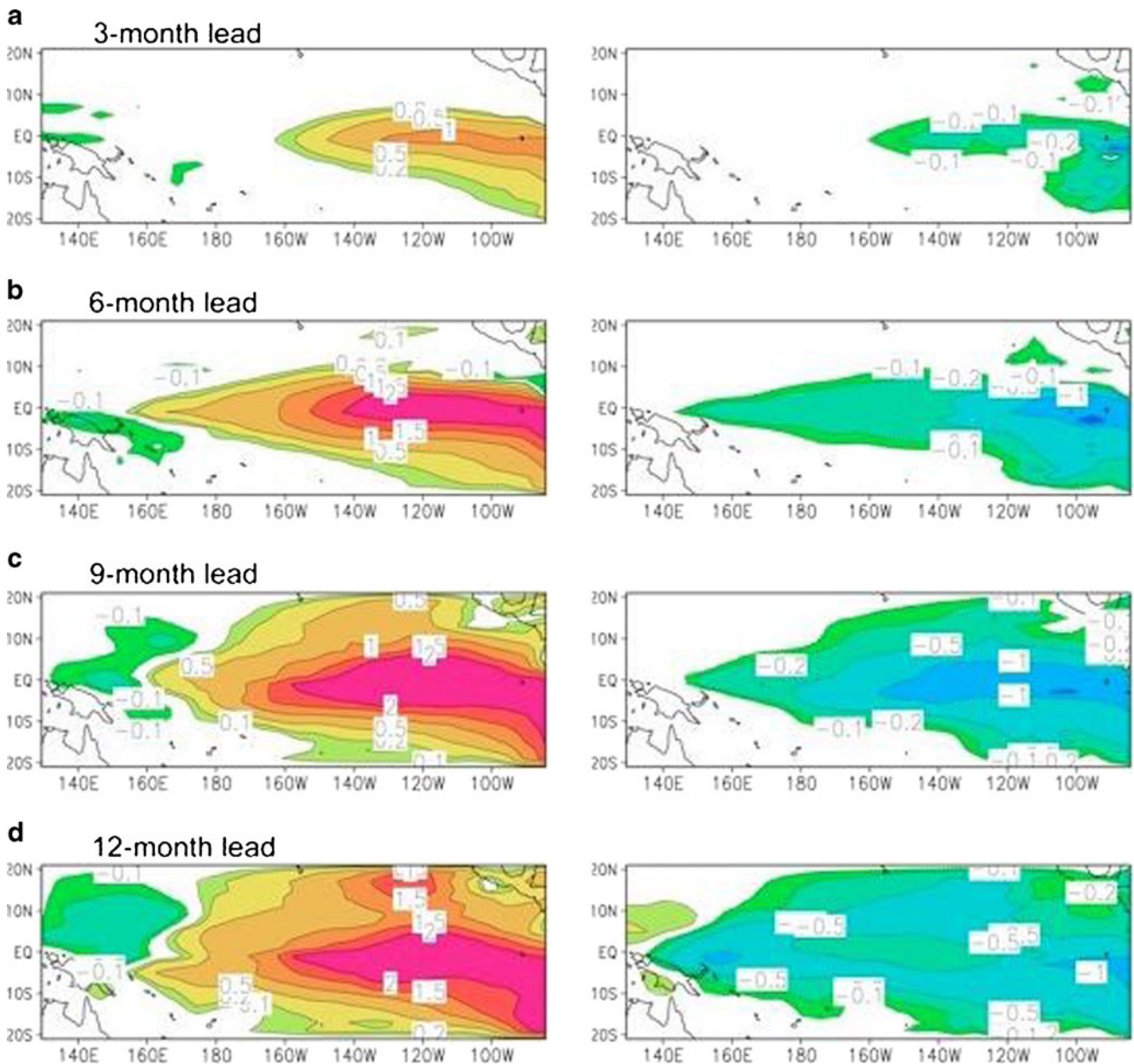


Fig. 2 The time evolutions of SSTA component with lead times of 3, 6, 9, and 12 months for the OPR triggered El Niño (a) and La Niña (b) events with the starting month being January

chosen norm do not exceed 1.0 (dimensional SSTA 2 °C and thermocline depth anomaly 50 m, respectively).

Yu et al. (2009) pointed out that CNOP errors can be classified into two types by means of cluster analysis and found that one type of CNOP error causes positive prediction error of Niño-3 index and the other type leads to negative. Hence, in this study based on the new reference El Niño state triggered by the OPRs, 48 initial errors (24 global CNOP errors and 24 local CNOP errors) are classified into two types of OGEs according to the sign of prediction error of the Niño-3 index. It is found that 22 errors have caused the difference in Niño-3 indices achieving the

maximum positive values, which are termed as a type 1 OGEs. The other 26 initial errors have caused negative values of prediction errors of Niño-3 indices and are termed as a type 2 OGEs. The spatial structure of the composite type 1 OGEs (Fig. 3a) shows a rather similar structure to that of the composite OPRs for El Niño in Fig. 1, with negative SSTA errors in the equatorial central Pacific and positive SSTA errors in the equatorial eastern Pacific, plus positive thermocline depth errors in the entire equatorial Pacific. Type 2 OGEs resemble the type 1 OGEs, but with the opposite sign (Fig. 3b), causing the underestimate of the Niño-3 index during the El Niño event.

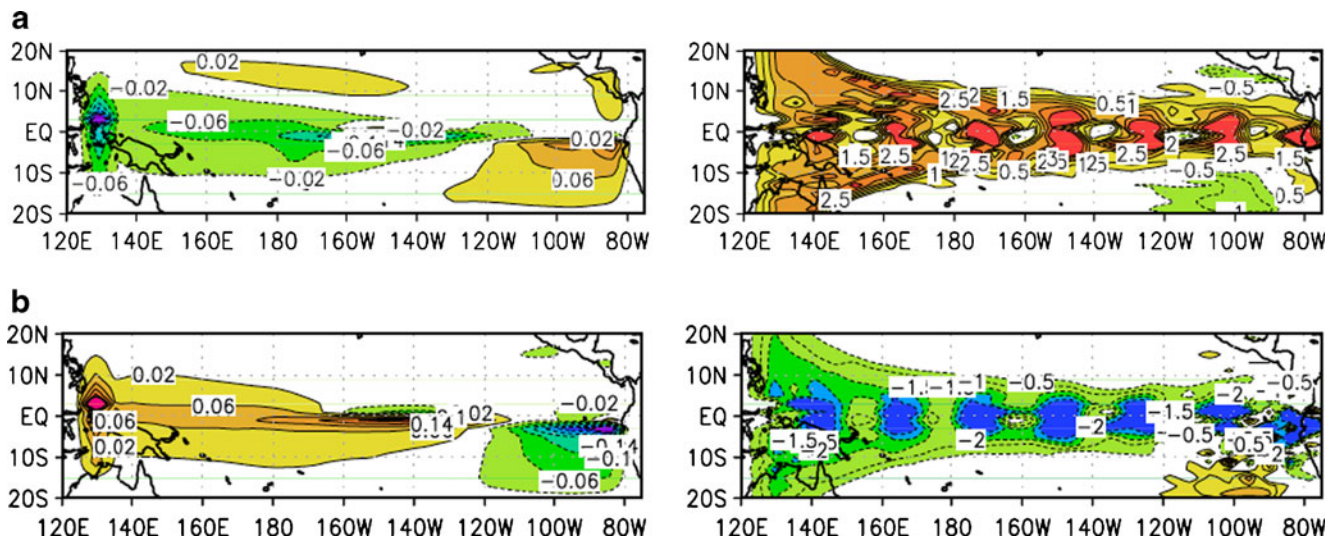


Fig. 3 The composite type 1 OGE (a) and type 2 OGE (b) with SSTA (left) and thermocline depth anomalies (right)

Yu et al. (2009, 2012) reported that the physics of the OGE can be explained by the same mechanism and that Bjerknes positive feedback is responsible for the error growth. The OGE, located in the equatorial central and eastern Pacific with a dipole pattern, acts as a trigger of Bjerknes positive feedback. Weaker (stronger) easterly trade winds over the dipole induce downwelling (upwelling) Kelvin waves that act to weaken (intensify) the upwelling in the equatorial eastern Pacific, where the shallow thermocline favors thermocline–SST feedback. Consequently, the positive (negative) OGE of SSTA in the Niño-3 region is amplified, causing a significant prediction error of Niño-3 indices and resulting in overestimation (underestimation) of the strength of El Niño events. Figure 4 shows the evolutions of the composite SSTA component for type 1 OGEs and type 2 OGEs associated with the El Niño events predictions. The two different behaviors of error growth related to the El Niño event are very similar to those optimal precursors obtained for the El Niño and La Niña events.

2.3 Similarities between the OPR and OGE

To further examine the relationship between the OPRs and OGEs, we adopted the similarity coefficient s to quantify the degree of similarity, which is defined as

$$s = \frac{\langle (Th)_\alpha, (Th)_\beta \rangle}{\| (Th)_\alpha \| \cdot \| (Th)_\beta \|}, \tag{2}$$

where $\|Th\|^2 = \sqrt{\sum_{i=1}^m \sum_{j=1}^n (T_{i,j})^2 + (h_{i,j})^2}$ which integrates over the domain, and $(Th)_\alpha = (T_{ij}^\alpha, h_{ij}^\alpha)_{m \times 2n}$, $(Th)_\beta = (T_{ij}^\beta, h_{ij}^\beta)_{m \times 2n}$ represent the OPR and OGE field as a vector. Based on the above formula, s ranges from -1 to 1 .

It is found that the OPRs which trigger the El Niño onset have a positive correlation with type 1 OGEs and negative correlation with the type 2 OGEs. The similarity indices between the composite OPRs for El Niño events and type 1 OGEs/type 2 OGEs are 0.62 and -0.60 , respectively. It is clear that the similarity between the optimal precursors and the optimally growing initial error is very high.

The main reason why the OGE share the similar pattern with the OPR might be that the evolution of OGE can also be explained by the Bjerknes positive feedback, which is responsible for the evolution of OPR. The only difference is that the two perturbations, OPR and OGE, are superimposed on different reference states, one being the annual cycle and the other the annual cycle plus an El Niño event. However, the magnitude of El Niño event is relatively much smaller than that of the annual cycle in the reference state for the computation of OGE, and is not capable of seriously affecting the evolution of perturbation superposed on the reference state. This feature makes the OPR and OGE share a similar pattern in the central and eastern Pacific in terms of the spatial pattern of SSTA. Due to the existence of the easterly trade winds along the equator and the resultant mean upwelling in the eastern Pacific, the thermocline is shallower in this region than within the equatorial western Pacific. The shallower thermocline in the equatorial eastern Pacific favors the influence of a variable thermocline on the development of SSTA by means of upwelling or downwelling. It is supposed that the space-dependent climatological mean thermocline depth enables the dipole pattern of the SSTA, existing in both OPR and OGE, appearing in the central and eastern Pacific. Although, the reference state of thermocline depth for the OGE could be a little deeper than that for the OPR due to the superimposed El Niño event, it is still advantage for the evolution of perturbation in the central and eastern Pacific.

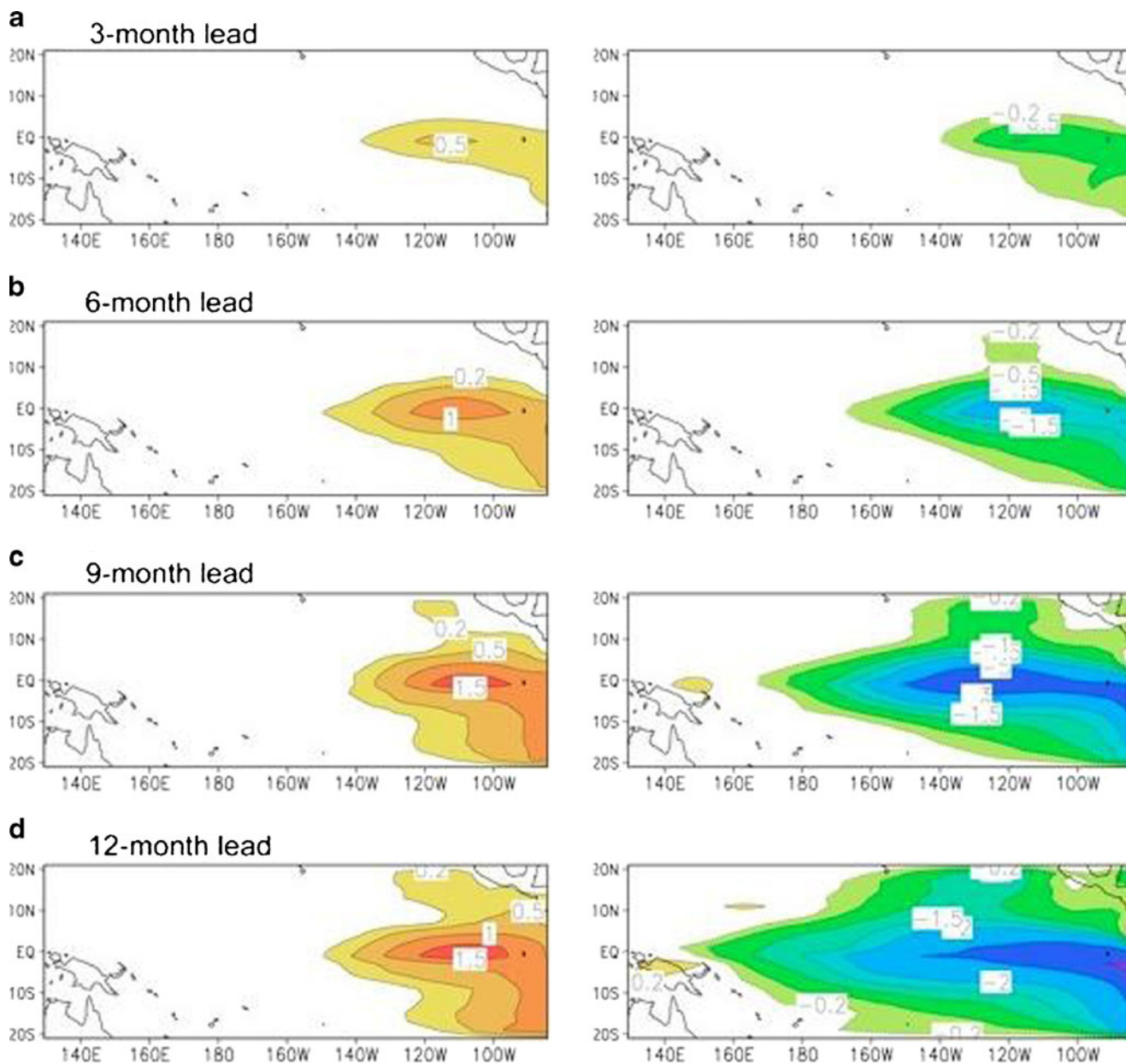


Fig. 4 The time evolutions of composite SSTA component with lead times of 3, 6, 9, and 12 months for type 1 OGEs (*left*) and type 2 OGEs (*right*)

3 Implications of similarities between OPRs and OGEs in targeted observation

In the past decade, the use of targeted observations to improve the numerical forecasts of the high-impact weather events has been examined in a series of field programs (see Langland 2005 for an overview of targeting programs and relevant references). The improved observation network will be helpful in detecting signals and reducing the observation errors existing in numerical forecasts. A key problem in observation targeting is the determination of the sensitive area where additional observations are expected to yield a better forecast than observations taken in other regions.

Morss and Battisti (2004a, b) suggested that for ENSO forecasts longer than a few months, the most important area for observations is the eastern equatorial Pacific, south of the equator; a secondary region of importance is the western equatorial Pacific. We have shown that large values of the OPR in the equatorial central and eastern Pacific evolve into strong ENSO events. This finding raises the possibility of improving the forecast skill by detecting the initial perturbation within the sensitive area (equatorial eastern Pacific), which could be achieved by additional targeted observations in this area.

To evaluate the importance of sensitive area defined by OPR, we next examine the extent to which the prediction

results are affected when OPR are only precisely observed in a particular area while not captured in other areas. We have adopted the similar approach as in Yu et al. (2012). To examine the effect of the optimal perturbation in different areas on prediction, for each OPR six subsets are generated by adding on its component in domain i ($i=1 \dots 6$, Fig. 5, same as in Yu et al. 2012) instead of the full OPR. For each OPR (including the SSTA and the thermocline depth anomaly components), six sets of numerical experiments are then performed with these new initial perturbation fields, accordingly they are denoted by *Exp i*. Prediction results (i.e., the evolution of the Niño-3 SST deviations from the basic run for which no perturbation field was added on) caused by each set of new experiment are computed for *Exp i* and then averaged over the four initial times (January, April, July, October). The averaged Niño-3 SSTA evolutions for the six sets of new experiment are plotted in Fig. 6. By superimposing the initial perturbation in the sensitive area (Domain 5), without adding any perturbation field in the other regions, the Niño-3 SSTA has the strongest growth after 1 year in *Exp 5* (purple line). It is found that adding in the initial perturbation in any of the other five areas would not cause El Niño occurrence in prediction. Therefore, if the initial perturbations in the sensitive area are not detected at the initial time, it will affect the prediction result significantly, regardless of whether the initial perturbation is observed in any of the other areas.

Meanwhile Yu et al. (2012) also identified the sensitive area (equatorial eastern Pacific) for ENSO prediction by CNOP method. They have performed a series of experiments showing that the sensitive area determined by the OGE is the region where the initial errors tend to grow most strongly and fast, and eventually evolve into the worst prediction case. Their findings suggest that by eliminating

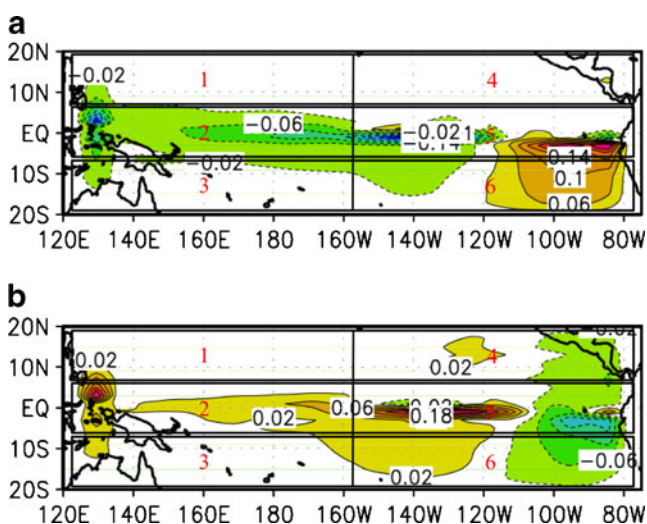


Fig. 5 Two types of composite OPRs (a, b) shown in six rectangular domains denoted by Domain i ($i=1, \dots, 6$). Large values of both types of OPRs occur mainly in Domain 5

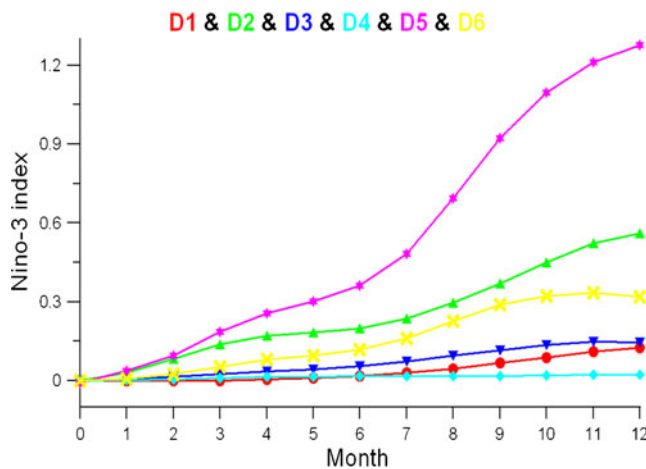


Fig. 6 The Niño-3 SSTA evolution caused by the six subsets of initial perturbations averaged over the four initial times. The six subsets of new initial perturbations are generated by adding in its components in one particular domain of the six from the original initial perturbation field

the initial errors of SSTA in the sensitive area (Domain 5), without changing the initial errors of SSTA in other regions, the prediction results can be significantly improved.

The results of the current study have demonstrated that the main location of optimally precursors for ENSO events overlaps with that of the sensitive areas where initial errors are found to grow optimally. Given the high cost of observations over ocean, a focus on a localized sensitive area may represent an economical and efficient strategy in terms of targeted observations with the aim of improving the prediction skill of ENSO. With the properties of localization and high similarities between ENSO precursors and optimally growing initial errors in SSTA over the equatorial central and eastern Pacific, we may implement the targeted observations in such regions in advance to improve the ENSO prediction to the greatest extent possible. On one hand, decreasing the initial errors in the sensitive area may help avoid the largest negative effect by OGE on ENSO predictions. On the other hand, an improved observation network will be helpful in the detection of signals provided by the precursor triggering ENSO events and avoiding false El Niño predictions.

4 Conclusion

In this study, the conditional nonlinear optimal perturbation method is adopted to investigate the similarities between the OPRs for ENSO events and the OGEs for ENSO prediction. The Zebiak–Cane model is used to simulate the ENSO event. This model might be relatively simple and may not consider the complete physics of coupled ENSO mechanisms, nonetheless the model is capable of capturing the key characteristics and the variability associated with ENSO. To seek the initial perturbation that is most likely to develop into an ENSO

event, the ZC-specified climatology with the seasonal cycle is used as the basic state. The El Niño events triggered by these OPRs are chosen as the basic state to seek the OGEs that cause the largest prediction errors.

The model simulations show that both the OPR and OGE have the properties of localization, involving the longitudinal dipole of SSTA over the equatorial Pacific and the relatively uniform thermocline depth anomalies in the equatorial Pacific. The composite OPRs for El Niño events comprise negative SSTA perturbations in the equatorial central Pacific and positive SSTA in the equatorial eastern Pacific, plus positive thermocline depth perturbations in the entire equatorial Pacific (opposite for OPRs for La Niña events). The spatial structure of composite OPRs for El Niño events shows positive correlations with the type 1 OGEs for the El Niño event triggered by the OPRs, and negative correlations with type 2 OGEs, which are classified based on the resultant sign of Niño-3 indices at the prediction time. The plausible reason why the OGEs share the similar pattern with the OPRs might be that the evolution of both OGEs and OPRs can be explained by the Bjerknes positive feedback. This similarity implies that if we implement the targeted observations in the obtained CNOP area, not only can the optimally growing initial errors in El Niño prediction be significantly eliminated, but also the signals provided by precursors triggering ENSO onset can be easily captured.

Acknowledgments This work was jointly sponsored by the National Basic Research Program of China (nos. 2012CB417404, 2012CB417403, 2010CB950402), the National Nature Scientific Foundation of China (no. 41230420), the Knowledge Innovation Program of the Chinese Academy of Sciences (no. KZCX2-EW-201), the National Nature Scientific Foundation of China (nos. 41006007), and the Basic Research Program of Qingdao Scientific and Technological Plan (111495jch).

References

- Birgin EG, Martinez JM, Raydan M (2000) Nonmonotone spectral projected gradient methods on convex sets, *SIAM J. Control Optim* 10:1196–1211
- Blumenthal MB (1991) Predictability of a coupled ocean–atmosphere model. *J Climate* 4:766–784
- Buizza R, Palmer TN (1995) The singular-vector structure of the atmospheric general circulation. *J Atmos Sci* 52:1434–1456
- Chen YQ, Battisti DS, Palmer RN, Barsugli J, Sarachik E (1997) A study of the predictability of tropical Pacific SST in a coupled atmosphere/ocean model using singular vector analysis. *Mon Wea Rev* 125:831–845
- Duan WS, Mu M, Wang B (2004) Conditional nonlinear optimal perturbations as the optimal precursors for El Niño–Southern Oscillation events. *J Geophys Res* 109:D23105. doi:10.1029/2004JD004756
- Duan W, Wei C (2012) The ‘spring predictability barrier’ for ENSO predictions and its possible mechanism: results from a fully coupled model. *Int J Climatol*. doi:10.1002/joc.3513
- Langland RH (2005) Issues in targeted observing. *QJR Meteorol Soc* 131:3409–3425. doi:10.1256/qj.05.130
- Lorenz EN (1965) A study of the predictability of a 28-variable atmospheric model. *Tellus* 17:321–333
- Molteni F, Buizza R, Palmer TN, Petroliagis T (1996) The new ECMWF ensemble prediction system: methodology and validation. *QJR Meteorol Soc* 122:73–119
- Moore AM, Kleeman R (1996) The dynamics of error growth and predictability in a coupled model of ENSO. *QJR Meteorol Soc* 122:1405–1446
- Moore AM, Kleeman R (1997a) The singular vectors of a coupled ocean–atmosphere model of ENSO, Part I: thermodynamics, energetics and error growth. *QJR Met Soc* 123:953–981
- Moore AM, Kleeman R (1997b) The singular vectors of a coupled ocean–atmosphere model of ENSO, Part II: sensitivity studies and dynamical interpretation. *QJR Met Soc* 123:983–1006
- Moore AM, Vialard J, Weaver A, Anderson DLT, Kleeman R, Johnson JR (2003) The role of atmospheric dynamics and nonnormality in controlling optimal perturbation growth in coupled models of ENSO. *J Clim* 16:951–968
- Morss RE, Battisti DS (2004a) Evaluating observing requirements for ENSO prediction: experiments with an intermediate coupled model. *J Climate* 17:3057–3073
- Morss RE, Battisti DS (2004b) Designing efficient observing networks for ENSO prediction. *J Climate* 17:3074–3089
- Mu M, Duan WS (2003) A new approach to studying ENSO predictability: conditional nonlinear optimal perturbation. *Chin Sci Bull* 48:1045–1047
- Mu M, Duan WS, Wang B (2003) Conditional nonlinear optimal perturbation and its applications. *Nonlinear Processes Geophys* 10:493–501
- Mu M, Zhang ZY (2006) Conditional nonlinear optimal perturbation of a barotropic model. *J Atmos Sci* 63:1587–1604
- Mu M, Xu H, Duan WS (2007) A kind of initial errors related to ‘spring predictability barrier’ for El Niño events in Zebiak–Cane model. *Geophys Res Lett* 34:L03709. doi:10.1029/2006GL027412
- Mureau R, Molteni F, Palmer TN (1993) Ensemble prediction using dynamically-conditioned perturbations. *QJR Meteorol Soc* 119:299–323
- Philander SGH (1990) *El Niño, La Niña, and the southern oscillation*. Academic Press, San Diego, p 289
- Thompson CJ (1998) Initial conditions for optimal growth in a coupled ocean–atmospheric model of ENSO. *J Atmos Sci* 55:537–557
- Xu H (2006) Studies of predictability problems for Zebiak–Cane ENSO model. PhD Thesis, Beijing, Institute of Atmospheric Physics
- Xu H, Duan WS (2008) What kind of initial errors cause the severest prediction uncertainty of El Niño in Zebiak–Cane model. *Adv Atmos Sci* 25:577–584
- Xue Y, Cane MA, Zebiak SE, Blumenthal MB (1994) On the prediction of ENSO: a study with a low-order Markov model. *Tellus* 46A:512–528
- Xue Y, Cane MA, Zebiak SE (1997a) Predictability of a coupled model of ENSO using singular vector analysis. Part I: optimal growth in seasonal background and ENSO cycles. *Mon Wea Rev* 125:2043–2056
- Xue Y, Cane MA, Zebiak SE (1997b) Predictability of a coupled model of ENSO using singular vector analysis. Part II: optimal growth and forecast skill. *Mon Wea Rev* 125:2057–2073
- Yu Y, Duan WS, Mu M (2009) Dynamics of nonlinear error growth and season-dependent predictability of El Niño events in the Zebiak–Cane model. *QJR Meteorol Soc* 135:2146–2160
- Yu Y, Mu M, Duan W, Gong T (2012) Contribution of the location and spatial pattern of initial error to uncertainties in El Niño predictions. *J Geophys Res*. doi:10.1029/2011JC007758
- Zebiak SE, Cane A (1987) A model El Niño–southern oscillation. *Mon Weather Rev* 115:2262–2278